Acoustical Physics, Vol. 50, No. 2, 2004, pp. 222–231. Translated from Akusticheskiĭ Zhurnal, Vol. 50, No. 2, 2004, pp. 272–282.

Heating of Biological Tissues by Two-Dimensional Phased Arrays with Random and Regular Element Distributions

E. A. Filonenko*, L. R. Gavrilov, V. A. Khokhlova*, and J. W. Hand*****

** Moscow State University, Vorob'evy gory, Moscow, 119899 Russia*
e-mail: vera@acs366.phys.msu.su
*** Andreev Acoustics Institute, ul. Shvernika 4, Moscow, 117036 Russia*
e-mail: gavrilov@akin.ru
**** Hammersmith Hospital, Imperial College, London, W12 0HS United Kingdom*
Received May 28, 2003

Abstract—The effect of an irregularity of the element distribution in a two-dimensional phased array upon the efficiency of heating of biological tissue is studied in an ultrasonic surgery regime. Two arrays of 256 piston elements, which either form a regular square pattern or are positioned randomly on the surface of a spherical segment, are considered as a model. The formation and the steering of a set of nine foci along the array axis and in the direction perpendicular to it are investigated. The theoretical model includes the algorithm of determining a phase set at the array elements that is optimal for the formation of foci with equal intensities and a preset geometry, as well as the calculation of acoustic and temperature fields in a tissue. The results of numerical simulation are presented for the spatial distributions of ultrasonic intensity, temperature, and the corresponding thermal dose in tissue. It is demonstrated that an irregularity of the element distribution reduces the level of secondary intensity peaks in the field produced by the array. This provides an opportunity to avoid the overheating and ablation of tissue outside the target volume, even in the case of steering with the set of foci away from the array axis within a distance of ±7 mm. A nine-foci regime is studied with the parameters necessary to produce uniform thermal ablation in a volume that is evaluated on the basis of the thermal dose distribution. © *2004 MAIK "Nauka/Interperiodica".*

Opportunities to use phased arrays capable of focusing ultrasonic energy and electrically steering the focus within a preset volume of a biological tissue have been actively investigated in connection with the development of new noninvasive surgery methods [1–9]. An advantage of phased arrays is their capability to simultaneously produce several foci in tissue and in this way increase the volume of the affected region, which essentially reduces the treatment time [2]. However the discrete structure of an array can give rise to undesirable sidelobes and secondary peaks in the acoustic field produced by the array [3–6]. It is known that the steering of foci in the direction perpendicular to the axis of a regular array within a distance of 7–10 mm leads to the appearance of secondary peaks with an intensity level reaching 50–60% of the maximum intensity in the major foci [8]. In the case of greater distances, the secondary intensity peaks may be still higher. The problem of secondary peaks in the field of phased arrays is especially important for ultrasonic surgery, where high intensity values (500–3000 W/cm^2) are used, which lead to a fast temperature rise in the focal region (above 60–80°C) within several seconds. This regime can be used for the ablation of tumors in soft tissues and also to stop internal bleeding [10]. A series of papers [2–6] are devoted to discussing the problem of secondary peaks in the acoustic field of therapeutic arrays and the ways to minimize the overheating of tissue along the path of ultrasound propagation to the target region.

One of the approaches used to reduce the level of secondary peaks is based on the utilization of arrays with elements positioned randomly on their surfaces [7–9]. This approach is also known in radar [11], where, however, the effect of randomization does not manifest itself as noticeably as in the case of powerful acoustic arrays. This can be explained by the fact that the velocity of light is greater than the velocity of sound, and, therefore, it is much simpler to manufacture an electromagnetic array with a distance between the centers of neighboring elements not exceeding the half-wavelength $\lambda/2$. Manufacturing such an acoustic array, which in addition has an acoustic power not smaller than 300–500 W, requires an extremely large number of elements and channels feeding them. Therefore, the development of theoretical models and numerical algorithms for calculating and analyzing the acoustic field and the corresponding temperature distribution in tissue in the case of the utilization of arrays of various configurations is important for designing therapeutic arrays and planning an experiment. Numerical simulation and comparative analysis of acoustic [8, 9] and temperature [12] fields produced by two-dimensional phased arrays for the case of steering a single focus with the help of arrays with regular and random distri-

1063-7710/04/5002-0222$26.00

butions of 256 elements demonstrated that irregularity in the element distribution noticeably improves the quality of intensity and temperature distributions. A randomization of the element distribution suppresses the secondary intensity and temperature peaks in the field produced by the array and provides an opportunity to bring the size of the elements up to five sound wavelengths while still retaining an acceptable intensity level for the secondary peaks (approximately 10% of the principal peak in the case of steering a single focus up to 15 mm away from the array axis) [8, 9, 12]. An increase in the size of elements leads to a sharp decrease in the effect of randomization of element distribution. For example, elements with a diameter of 11.2λ were used in [7], and the effect of randomization was insignificant.

Here, we investigate the regime of simultaneous formation and steering of nine foci ($N = 9$) by a powerful acoustic array with random and regular element distributions on the array surface shaped as part of a sphere (Fig. 1). The theoretical model presented below includes an algorithm for calculating the coordinates of element positions for a random array, for choosing the phases at the elements to produce foci of equal intensities, and for calculating the acoustic and temperature fields in tissue, as well as the distribution of the thermal dose. Modeling and analysis of the acoustic field and thermal sources and the spatial distributions of temperature and thermal dose are performed for arrays with regular and random element distributions in the case of steering the focal volume along the array axis and in the direction perpendicular to it. The necessary parameters of irradiation and focus geometries that provide tissue ablation not only locally, in each focal region, but also uniformly in the whole volume between them are revealed.

Let us consider the problem of obtaining nine foci at a preset distance z at the array axis, so that these foci form a square pattern in the (x, y) plane perpendicular to the z axis and that the distance between the focus centers is, foe example, 3 mm (Fig. 2). To estimate the array capability to steer the set of foci along the array axis and in the direction perpendicular to it, we set the shift of the central focus along the array axis (z axis) to be equal to 2 cm from the geometrical focus toward the array and equal to 0.7 cm in the y direction away from the axis. It is assumed that ultrasound propagates in a tissue with the following acoustic parameters: density $\rho_0 = 1000$ kg/m^3, sound velocity $c_0 = 1500$ m/s, and attenuation coefficient $\alpha_0 = 5$ m^{-1} at a frequency of 1 MHz, with the attenuation coefficient increasing linearly with frequency.

We use an acoustic array of $M = 256$ circular piston elements with diameters $d = 5$ mm and operating frequency $f_0 = 1.5$ MHz. The elements are distributed over the surface of a spherical segment 13 cm in diameter with a curvature radius $F = 12$ cm. The maximum distance between the centers of the outermost elements is 12 cm.

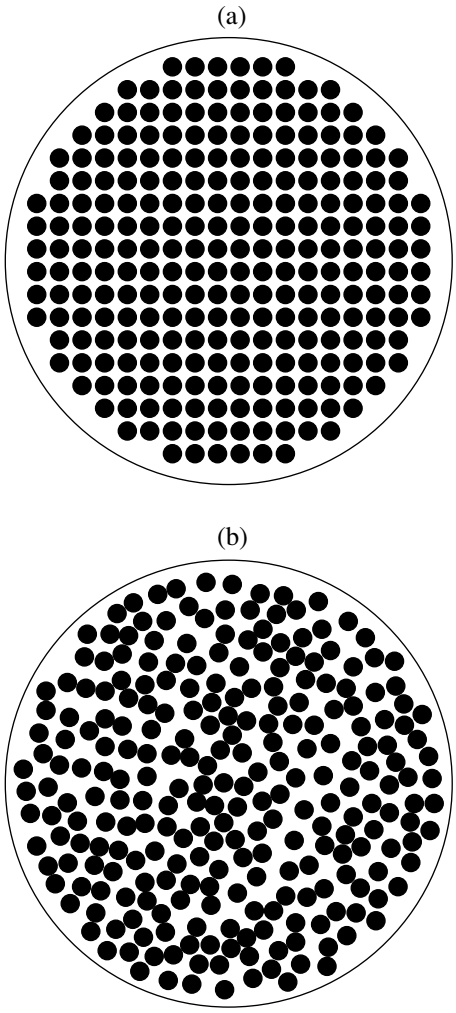

Fig. 1. Schematic diagrams of ultrasonic arrays containing 256 elements 5 mm in diameter: (a) a regular arrangement of elements in a square pattern and (b) a random distribution of elements over the array surface.

In the case of a regular array, the elements are positioned in squares with a distance of 6 mm between the centers of neighboring elements (Fig. 1a). A distribution in the form of a square pattern was selected because it is the most popular one among the designs of powerful therapeutic arrays discussed in the literature [4, 5].

In the case of a randomized array (Fig. 1b), the element coordinates are selected as follows. A large (tens of thousands) two-dimensional array of independent random coordinates (x, y) is formed with the help of a random-number generator (uniform distribution) in the interval from –6 to 6 cm. The coordinates within a circle with a radius of 6 cm are selected from it. The first point is chosen arbitrarily from this array at the beginning, and then all other 255 points (element coordinates) are chosen so as to be located no closer than 5.5 mm from all preceding ones. Coordinates inconsistent with this condition are rejected. In one of the realizations of element distributions obtained in this way

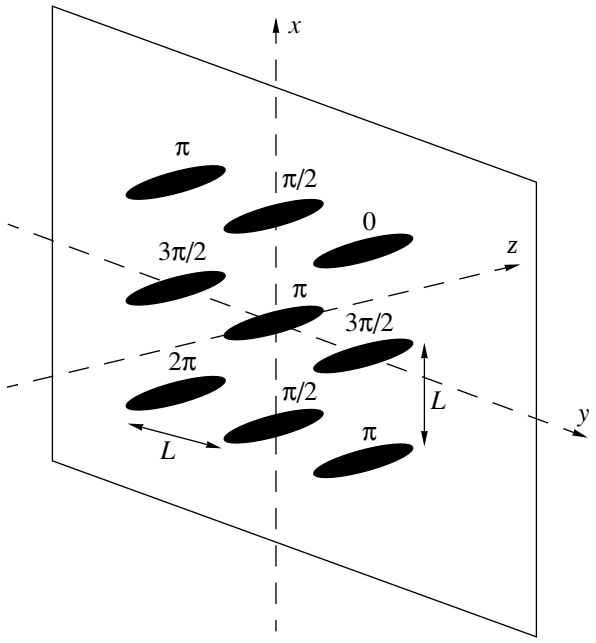

Fig. 2. Schematic diagram of nine foci in the *xy* plane and the method of rotation of the pressure phase at the foci. The distance between the foci L is equal to 3 mm.

and examined here (Fig. 1b), the distances between the centers of neighboring elements vary within the interval from 5.5 to 8.45 mm. It is necessary to note that the utilization of different sets of random coordinates of the 256 elements can affect the fine structure of the field produced by the array but does not influence in any way the main result: the use of randomized arrays leads to a considerable reduction of secondary intensity peaks caused by the regular discrete structure of the array.

Calculation of the acoustic field produced by an array in a tissue in the case of a preset element distribution and a set of control points (foci) in space can be conditionally divided into three stages: the calculation of the field of a single array element, the determination of the optimal phase set with a subsequent matching of the absolute values of amplitudes at the elements, and the determination of the array field by summation of all fields of all elements with the amplitude-phase distribution determined at the previous stages. At the first stage the acoustic field of one circular element of the array is calculated with the help of the Rayleigh–Sommerfeld integral [1, 13],

$$p(\mathbf{r}_i) = \frac{j\rho_0 c_0 k u_0}{2\pi}\int\limits_S \frac{\exp((jk-\alpha)|\mathbf{r}-\mathbf{r}_i|)}{|\mathbf{r}-\mathbf{r}_i|}dS, \qquad (1)$$

where p is the complex pressure amplitude, $k = 2\pi f_0/c_0$ is the wave number, $\alpha = 7.5\ \mathrm{m}^{-1}$ is the attenuation coefficient at the operating frequency of the array, u_0 is the amplitude of particle velocity at the element surface, $|\mathbf{r}-\mathbf{r}_i|$ is the distance from a point $\mathbf{r}$ of the radiating surface S of the circular piston element to the ith point in the space $\mathbf{r}_i$.

The Rayleigh–Sommerfeld integral (Eq. (1)) is calculated numerically at the nodes of a sufficiently dense spatial grid. The following values of simulation parameters are used: the integration region along the longitudinal coordinate is $2 < z < 16$ cm, the spatial window along the transverse coordinate is $0 < r < 10$ cm, and the grid step along both directions is $hz = hr = 0.2$ mm, which is 1/5 of the wavelength. For numerical integration, the element surface was divided into 7849 square regions with a side of 0.05 mm ($\lambda/20$), which provided the necessary precision of the solution. The solution obtained is further used to determine the phases at the elements and also in calculating the total field produced by the array.

At the second stage, the values of the complex amplitude of the particle velocity at each element are determined so as to obtain a set of $N = 9$ physical foci (control points) with preset coordinates in space. Additional conditions are imposed upon the selection of pressure amplitudes and phases at each control point: phases rotate uniformly clockwise with respect to the axis of the given set of foci with a step of $\pi/2$ (Fig. 2), and the values of the pressure amplitude at the control points are equal. The basis of the technique for calculating the complex amplitude of particle velocity at the elements was proposed in [1]. However, the brevity of its description makes it difficult to use it in practice. Therefore, below we give the basic components of this approach in two modifications. In one of them, the acoustic field of a piston element (Eq. (1)) is used for calculating the amplitude and phase of particle velocity at the elements [1]. In the second modification, the piston field is replaced by the field of a point source located at the element center [8, 9]. Both modifications are considered here to compare the resulting sets of phases and the acoustic fields produced by the array.

In the approximation of the linear propagation of an acoustic wave, the pressure $p(\mathbf{r}_n)$ at each nth control point ($n = 1, \ldots, N$) is the superposition of M partial pressures p_m produced by each of the M elements of the array, $p(\mathbf{r}_n) = \sum_{m=1}^{M} H_{nm}u_m$, or, in the matrix form,

$$P = H \times U. \qquad (2)$$

Here, u_m is the complex amplitude of particle velocity at the surface of the mth element ($m = \{1, \ldots, M\}$), U is the vector of the M values of the particle velocity amplitudes u_m, P is the vector of pressures $p(\mathbf{r}_n)$ at N control points, and the matrix H with the dimension $(N \times M)$ determines the operator of direct propagation from the mth element at the array to the nth control point in space. If the field of a piston element with a uniform distribution of particle velocity is used to solve Eq. (2), the elements of the matrix H_{nm} are determined by solution (1) that is calculated for the mth element of the

array at the *n*th control point:

$$H_{nm} = \frac{j\rho_0 c_0 k}{2\pi}\int\limits_{S_m}\frac{\exp((jk-\alpha)|(\mathbf{r}_m-\mathbf{r}_n)|)}{|\mathbf{r}_m-\mathbf{r}_n|}dS_m. \quad (3)$$

It should be noted that, to determine the values of the elements of the matrix H_{nm} (Eq. (3)), it is necessary to calculate the Rayleigh–Sommerfeld integral *NM* times (in *N* foci from *M* elements of the array). However, it is possible to use field (1) calculated for one of the elements to determine the matrix elements (3) from an arbitrary element *m* at an arbitrary control point *n*. To do this, we determine the position of the control point with respect to the cylindrical coordinate system connected with the selected element and determine the weighted mean value of the field at the closest nodes if the point lies within the intervals *hz* or *hr* of the grid. Multiplying the result by the complex amplitude of the particle velocity of the element, it is possible to obtain the value of the pressure field produced by the element *m* at the control point *n*.

However, if we use the field of a point source with the coordinate $\mathbf{r}_n$, the matrix elements H_{nm} have a simpler form:

$$H_{nm} = C\frac{\exp((jk-\alpha)|(\mathbf{r}_m-\mathbf{r}_n)|)}{|\mathbf{r}_m-\mathbf{r}_n|}, \quad (4)$$

where the coefficient of proportionality $C = j\rho_0 c_0 kS/2\pi$ is the same for all *n* and *m* and $S = \pi d^2/4$ is the area of the array element.

In the case of equal quantities of array elements and foci ($N = M$), the matrix *H* is quadratic, and there is a unique solution to the set of equations (2); i.e., $U = H^{-1} \times P$, where H^{-1} is the matrix inverse with respect to matrix *H*. Within the framework of this problem, an underdetermined system of equations ($N < M$) exists, which has an infinite number of solutions in the general case [14]. Therefore, the principal goal is to determine the "best" solution, i.e., a vector $\hat{U}$ with the elements $\hat{u}_m$ that provides the minimum acoustic power at the array (the minimum norm of vector $\hat{U}$) with the given values of complex pressure at the control points. From a physical point of view, this condition guarantees that the control points are local peaks of the field. Here, we use the singular value decomposition method and the technique of minimization of the norm to construct a solution [14]. The method of decomposition of a singular quantity provides an opportunity to obtain a matrix pseudo-inverse to *H*, while the technique of minimization of the norm allows us to choose the "best" pseudo-solution $\hat{U}$. In this case, a solution to Eqs. (2) can be written down as

$$\hat{U} = H^{*T}(H\,H^{*T})^{-1}P. \quad (5)$$

Here, H^{*T} is the matrix conjugate to *H*, for which the transposition procedure is performed. The solution given by Eq. (5) provides the minimum norm of the vector *U* of matrix equation (2) [14]. The matrix $H^{*T}(M \times N)$ determines the operator of inverse propagation of an acoustic wave from the *n*th control point in space to the *m*th element at the array surface. The physical significance of the operator $(H\,H^{*T})^{-1}$ (the $N \times N$ matrix inverse of the matrix $H\,H^{*T}$) lies in the fact that it introduces a correction to the directivity of the element's field before the procedure of reconstructing the field at the control points [1, 14]. If we ignore this operator in Eq. (5), the field at the control points is reconstructed inaccurately.

It is necessary to note that a certain limiting admissible value of the amplitude of particle velocity (or intensity) exists at the surface of the piezoelectric array elements, which makes its operation safe. In the solution given by Eq. (5), the modulus of the complex amplitude $\hat{u}_m$ is not the same for different elements; i.e., if the velocities at some elements are close to the maximum admissible value, they can be very small at other elements. In this case, the array efficiency [1]

$$\eta_A = 100\% \times \sum\nolimits_{m=1}^{M}|\hat{u}_m|^2/Nu_{\max}^2,$$

where $u_{\max}$ is the maximum amplitude of particle velocity at its elements, can be from 20 to 35% in the case of the generation of nine foci. It is clear that the maximum efficiency of the array can be obtained when all elements have the same amplitude. Therefore, this condition of the minimum norm of the vector *U* is relaxed, and the iteration procedure of amplitude equalizing is performed to increase the efficiency of (to optimize) the acoustic array. The notion of a weighted norm is introduced to perform such an optimization [14]:

$$\|\hat{U}\|_W = (\hat{U}^{*T}\,W\,\hat{U})^{1/2}, \quad (6)$$

where *W* is a positively defined diagonal matrix with the dimension $M \times M$. The condition of amplitude equality is realized by calculating the diagonal matrix elements of matrix *W* in the iterative procedure [1]. If *W* is a unit matrix, the determination of a weighted norm (6) exactly reproduces the determination of the Euclidean norm [14]. A solution to matrix equation (2) taking into account weighted norm (6) is written down in the form

$$\hat{U} = W\,H^{*T}(H\,W\,H^{*T})^{-1}P. \quad (7)$$

At the first step of the iterations, the diagonal matrix elements of the weight matrix *W* in Eq. (7) are assumed to be equal to unity, and the velocity vector $\hat{U}$ (Eq. (5)) is determined. The solution obtained is verified for uniformity of the distribution of velocity amplitude using the criterion of array efficiency. If solution $\hat{U}$ satisfies the condition $\eta_A \geq 99\%$, the iterations are stopped. If the condition is not satisfied, a redetermination of the

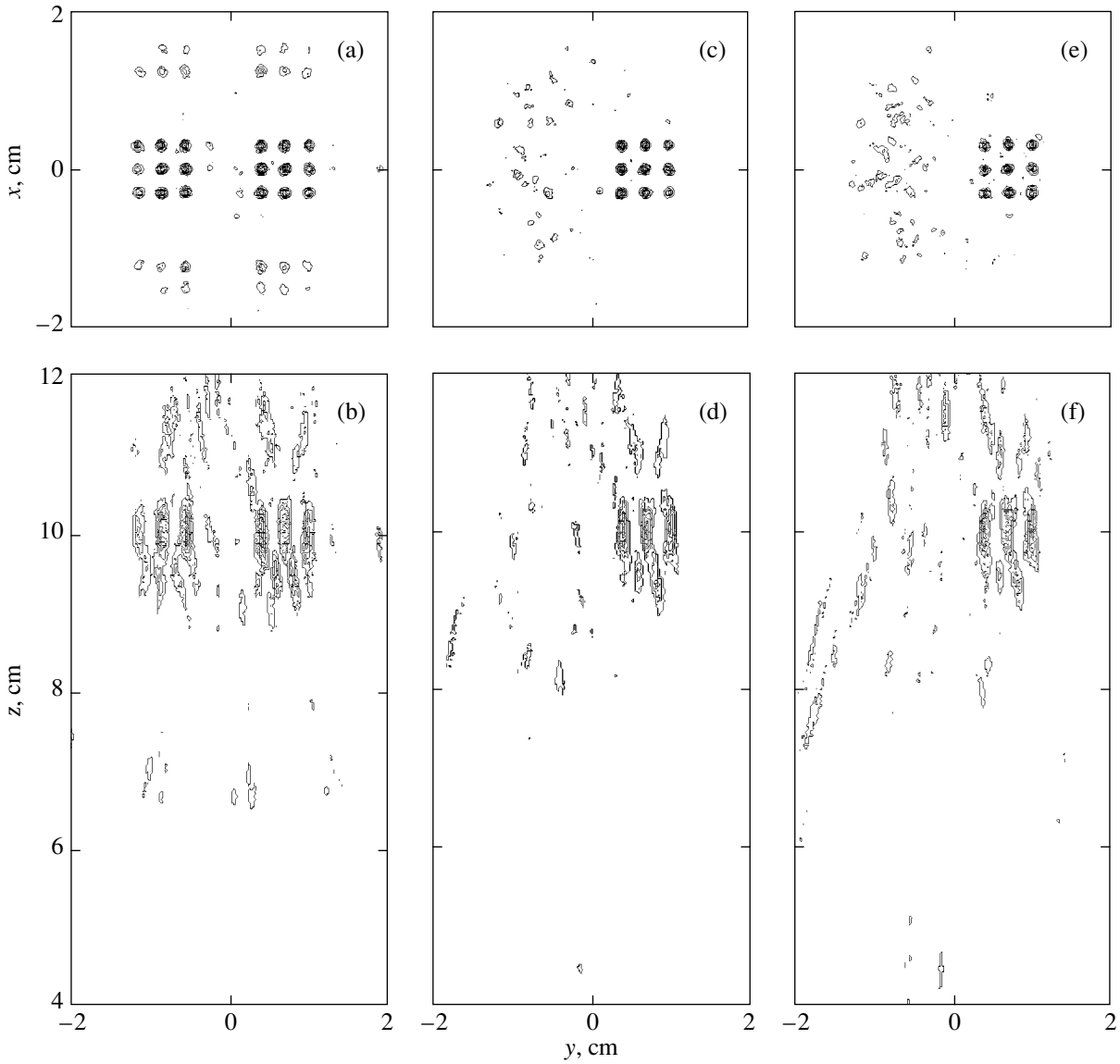

Fig. 3. Spatial intensity distributions in the *xy* plane (from above) and in the *yz* plane (from below) (a, b) for a regular array and (c, d) for two random arrays with a different choice of phases at the elements. Stirring with the set of foci is performed along the array axis to a distance of 2 cm from the geometrical focus towards the radiator and to 7 mm away from the axis. The intensity is normalized to the corresponding maximum value reached in the focus region.

diagonal elements of the weight matrix W takes place, so that $W_{mm} = u_{\max}/|\hat{u}_m|$ ($m = 1, \ldots, M$). Then, Eq. (7) is used again to calculate the vector of the complex amplitudes of particle velocity $\hat{U}$, taking into account the redetermined elements of the weight matrix. After that, the result is again tested to make sure it satisfies the condition $\eta_A \geq 99\%$. The described iteration technique provides an opportunity to conduct an equalization of the amplitude values of particle velocity at different elements on the array surface [1].

At the second stage, the pressure field in a tissue $\breve{p}(\mathbf{r})$ produced by the whole array is calculated for a selected value of amplitude and a preset distribution of phases of particle velocity at the elements. The calculation is performed in the nodes of a rectangular grid $\mathbf{r}_i$ with a step $hz = hy = hx = 0.2$ mm in the region $4 < z < 13$ cm along the array axis and $-2 < y < 2$ cm and $-2 < x < 2$ cm along the transverse coordinates. For this purpose, pressures from each element are determined analogously to the calculation of pressure at control points, which was described above, and the procedure of summation is performed (for details, see [8, 9]). The resulting pressure field is used to calculate the intensity field at the same grid in the plane wave approximation: $I(\mathbf{r}_i) = |\breve{p}(\mathbf{r}_i)|^2/2\rho_0 c_0$, and the field of thermal sources:

$$Q(\mathbf{r}_i) = 2\alpha I(\mathbf{r}_i), \tag{8}$$

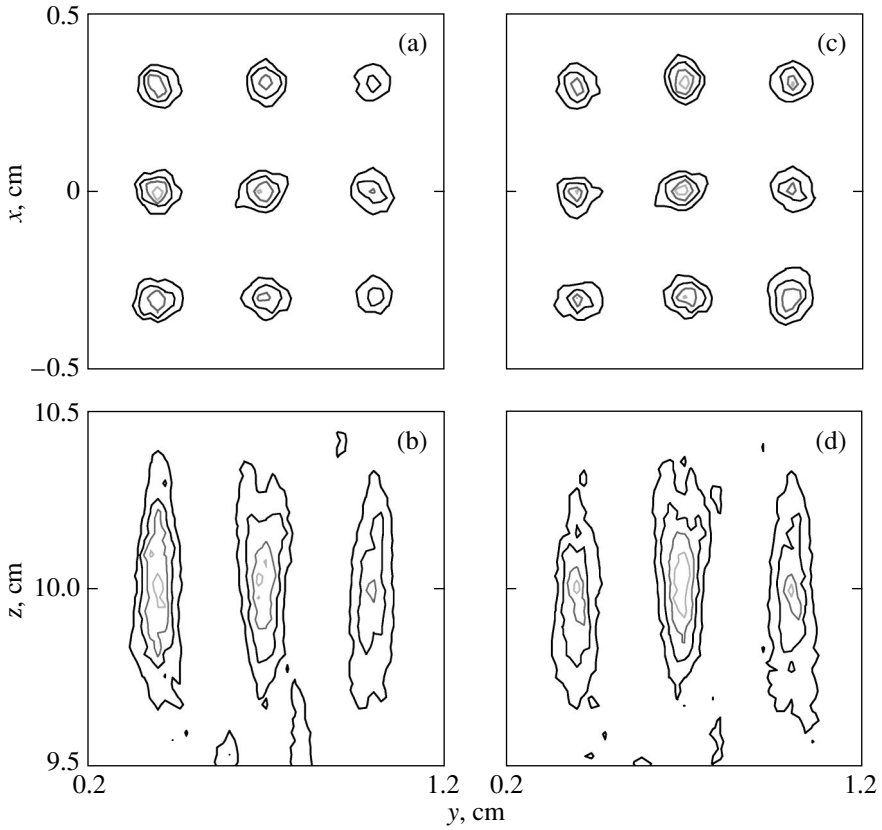

Fig. 4. Spatial intensity distributions (Fig. 3) for two random arrays on an extended scale. The phases of particle velocity at the elements are determined using either (a, b) the field of a point source or (c, d) the field of a piston element.

where the absorption coefficient at the operating frequency of the array is assumed to be equal to the attenuation coefficient α.

The inhomogeneous Pennes equation of heat conduction [15] is used to calculate the temperature field in a tissue:

$$\frac{\partial T}{\partial t} = k\Delta T - \frac{T - T_0}{\tau} + \frac{Q(\mathbf{r})}{c_v}, \qquad (9)$$

where $T = T(x, y, z, t)$ is the temperature in the tissue, $T_0 = 36.6$°C is the equilibrium temperature, $\Delta = \partial^2/\partial x^2 + \partial^2/\partial y^2 + \partial^2/\partial z^2$ is the Laplacian, $c_v = 3.81 \times 10^6$ W s/m^3 °C is the volumetric heat capacity, and $k = 1.33 \times 10^{-7}$ m^2/s is the thermal diffusivity. The perfusion time τ was selected to be sufficiently large, $\tau = 250$ s, so that the process of perfusion almost did not influence the heating of the tissue [16]. Equation (9) was solved numerically in the Cartesian coordinates (x, y, z) by the finite-difference method on the same spatial grid with the nodes where the acoustic field was calculated and the thermal sources Q were located. An algorithm developed earlier for a cylindrically symmetrical problem [17] and generalized here for the case of an arbitrary three-dimensional spatial distribution of a temperature field was used. The field was calculated within the region $4 < z < 13$ cm along the array axis and $-2 < y < 2$ cm and $-2 < x < 2$ cm along the transverse coordinates. At each time step of the grid $ht = 0.05$ s, the results for the temperature field were used to calculate the thermal dose [18]:

$$td_{T_{\text{ref}}} = \int_0^t R^{(T_{\text{ref}} - T_t)} dt, \qquad (10)$$

where the integration is performed over the total time of heating and subsequent cooling $t = t_{\text{heat}} + t_{\text{cool}}$ and T_{ref} is the temperature with respect to which the thermal dose necessary for thermal ablation of the tissue is calculated [18, 19]. In the hyperthermia regimes, the thermal dose usually corresponds to the temperature $T_{\text{ref}} = 43$°C maintained in the tissue during 120–240 min [20]. For heating regimes used in acoustic surgery, it is convenient to use $T_{\text{ref}} = 56$°C; then, the thermal dose $td_{T_{\text{ref}}} = 1$ s is equivalent to $td_{T_{\text{ref}}} = 140$ min at a temperature of 43°C [2, 18].

The results of the simulation given below provide an opportunity to investigate the influence of irregularity in the element distribution on the spatial distributions of thermal sources and the evolution of the temperature field and thermal dose in a tissue. As indicated above, the stirring of a set of nine foci was performed along the

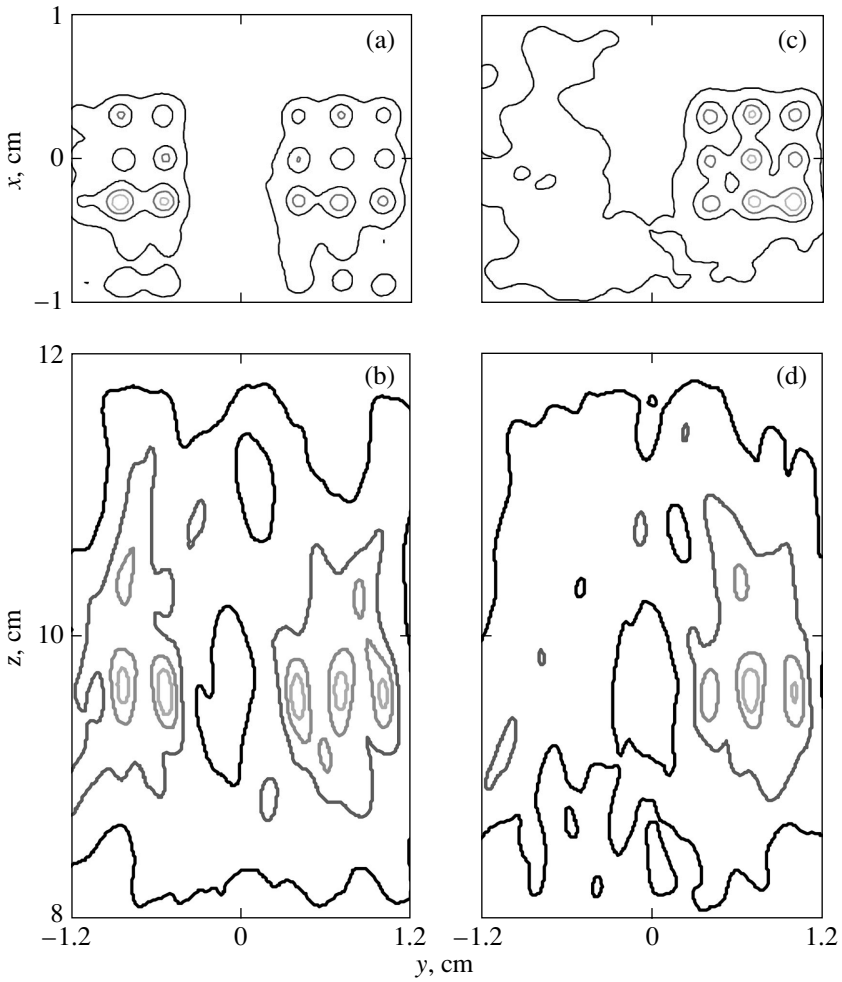

Fig. 5. Spatial temperature distributions after 8 s of heating in ultrasonic field (Fig. 3) with (a, b) regular and (c, d) random arrays. The phases at the elements are chosen with the help of the field of a piston element.

array axis to 2 cm from the geometrical focus towards the radiator and to 7 mm away from the array axis. Figure 3 demonstrates the spatial intensity distributions for regular (left) and random (in the middle and at the right of the figure) distributions of elements. The intensity was normalized to its maximum value I_{max} in the volume of the region of foci, and nine levels of contours in the figures correspond to an intensity change from $0.1I_{max}$ to $0.9I_{max}$. In the case of a regular array, the phases of particle velocities at the elements were reconstructed using the field of a point source located at the element center [8, 9]. In the case of a random array, both approaches were used, i.e., the approximation of a point source (the results are given in the middle of the figure) and the approximation of a piston element (at the right of the figure). The distributions are shown in two sections: *xy* at $z = 10$ cm (section from above) and *yz* at $x = 0$ (section from below). One can see that, in the case of using a regular array, an incidental set of pronounced secondary peaks with an intensity level exceeding 80% of I_{max} is observed together with the main set of physical foci (Figs. 3a and 3b). The presence of these secondary peaks is inadmissible, because they can lead to unpredictable heating of tissue outside the target region. If a randomized array is used, the intensity of the secondary peaks is considerably reduced down to a level below 30% of I_{max} (Figs. 3c–3f), which is more acceptable in practice. Figure 4 shows the same intensity distributions (on an extended scale) in the region of nine foci for a randomized array and for two approaches to the determination of phases at the elements. Four contours from $0.2I_{max}$ to $0.8I_{max}$ with the step between them equal to $0.2I_{max}$ are chosen for illustration.

The major differences in the intensity distributions obtained for a randomized array in the cases of choosing the phases at the elements in the approximations of point (Figs. 4a, 4b) or piston (Figs. 4c, 4d) sources are as follows. As can be seen from Fig. 3, in the first case (the approximation of a point source), the field does not contain any great number of secondary peaks with an intensity within 10–20% of I_{max}. In the second case (the

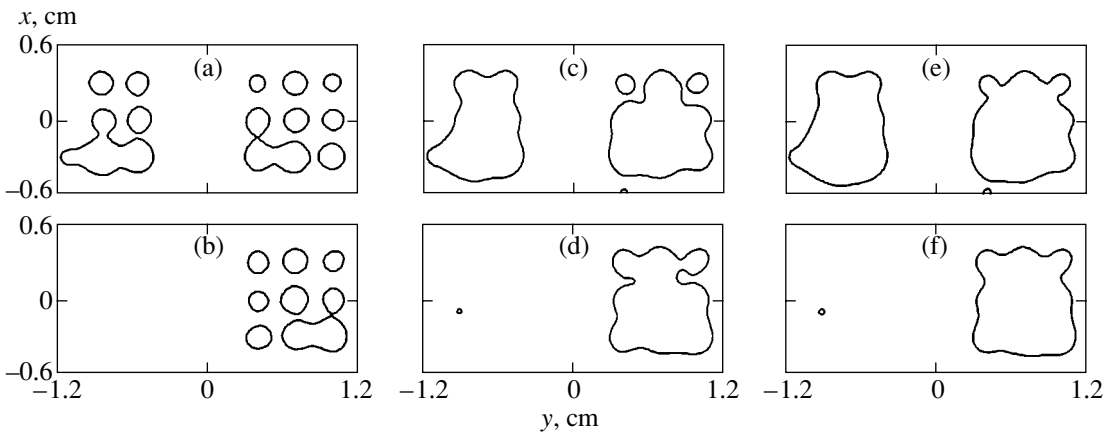

Fig. 6. Section in the *xy* plane for the thermal dose field (a, b) after 8 s of heating and later, after (c, d) 5 and (e, f) 10 s of cooling, for regular (above) and random (below) element distributions. The contour is drawn at a thermal dose level of $td_{T_{ref}} = 1$ s at a temperature of $T_{ref} = 56°C$ and encloses the region of thermal necrosis of tissue.

approximation of a piston element), a greater number of such peaks with the higher intensity of 10–30% of I_{max} is observed both along the array axis and in the transverse direction. However, the approach of a piston element is still preferable, because it provides an opportunity to obtain a set of nine foci with very close values of maximum intensity (Fig. 4). In the case of using the approximation of a point source, the intensity levels in the foci noticeably decrease with the distance from the array axis and constitute from 60–80% of I_{max} at the nearest foci to 40–60% of I_{max} at the foci most distant from the axis. Further calculation for a randomized array is conducted for the case of phase setting using the field of a piston element.

The simulation was performed for different intensities obtained at the foci, different distances between the foci, and different durations of treatment with the aim to determine a regime that provides a thermal necrosis of tissue after 5–10 s of treatment not only in the discrete number of regions around the foci but also in all intervals between them. Below, we present the results for a 8-s-long treatment and the geometry of focus arrangement already determined earlier, in determining the intensity fields (Figs. 2 and 3). The intensity at the radiator was selected to be 25 W/cm^2, which corresponded to a maximum intensity of 754 W/cm^2 in the focus region for a random array and an intensity of 845 W/cm^2 for a regular array. It is necessary to note that this high intensity value at the radiator is obtained under the assumption that ultrasound propagates in tissue through the whole distance from the array to the target depth of 10 cm. If the water–tissue boundary is located within 5 cm from the array, which is quite reasonable for many practical applications, the intensity at the radiator is 10.5 W/cm^2.

Figure 5 shows the spatial distributions of temperature in the same sections, *xy* and *yz*, as in Figs. 3 and 4 after 8 s of irradiation for regular (Figs. 5a, 5b) and random (Figs. 5c, 5d) distributions of elements. Four contours are presented, where the outer contour corresponds to the temperature exceeding the equilibrium value $T_0 = 36.6°C$ by $\Delta T = 0.2(T_{max} - T_0)$. The step between the contours is also equal to ΔT. Here, T_{max} is the maximum temperature value in the focal region, $T_{max} = 92.6°C$ and $\Delta T = 11.2°C$ for a regular array, and $T_{max} = 80.3°C$ and $\Delta T = 8.74°C$ for a random one. One can see that, in the temperature field of a regular array, the temperature increment in the incidental set of foci is not smaller but actually greater (Fig. 5a) than in the principal one, which is inadmissible for practical purposes. At the same time, in the case of a random array (Figs. 5c, 5d), one may expect that the ablation of tissue will occur only in the region where the set of nine foci is focused, because the temperature increment outside this region is much smaller.

Figures 6 and 7 demonstrate the evolution of thermal dose distributions for the same sections, *xy* and *yz*, selected above. The distributions are calculated for the time of 8 s corresponding to the moment of switching on ultrasound (Figs. 6a, 6b, 7a, 7b) and after 5 (Figs. 6c, 6d, 7c, 7d) and 10 s (Figs. 6e, 6f, 7e, 7f) after switching it off. The thermal dose fields obtained with regular (left) and random (right) arrays are compared. Contours in the figures correspond to the level of $td_{56} = 1$ s and surround the region of a thermal necrosis of tissue. As one can see, the role of thermal diffusion can be considerable even after the irradiation is switched off. Within 5 and 10 s after switching off the source, the outflow of heat from the strongly heated regions of foci to less heated regions occurs due to a high temperature gradient, which provides in this way the uniformity of ablation in the region between the foci. In the case of cooling times exceeding 10 s, no considerable changes in the thermal dose field are observed.

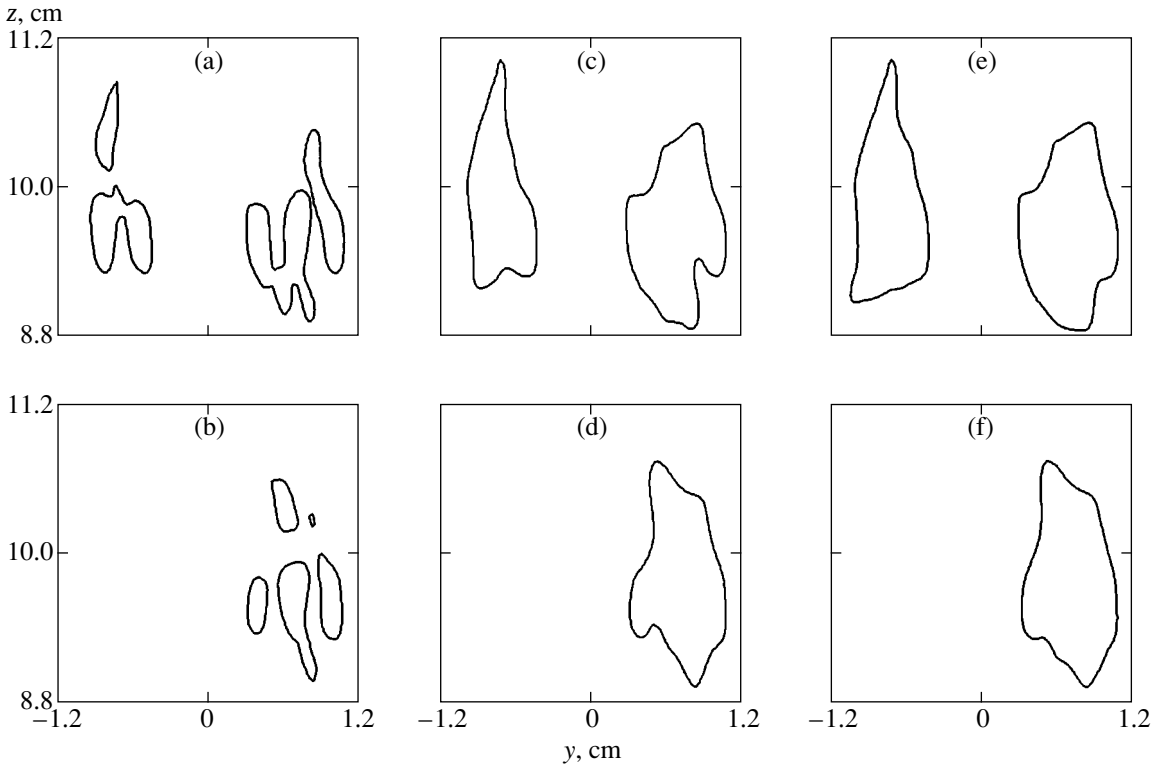

Fig. 7. Section in the *yz* plane for the thermal dose field (a, b) after 8 s of heating and later, after (c, d) 5 and (e, f) 10 s of cooling, for regular (above) and random (below) element distributions. The contour is drawn at a thermal dose level of $td_{T_{\mathrm{ref}}} = 1$ s at a temperature of $T_{\mathrm{ref}} = 56°\mathrm{C}$ and encloses the region of thermal necrosis of tissue.

To reduce the acoustic power of the array and the intensity values at the elements, the above-mentioned nine-foci regime can be modified to a regime with two sequentially switched sets of four and five foci formed at the same coordinates. The frequency of switching the sets can be selected within 10–20 Hz, as in [20]. The results of our calculation of the spatial distributions of acoustic and temperature fields, which correspond to this regime, show that, for obtaining the same thermal effect within the heated region, the array power and average intensity can be reduced almost twice (for brevity, we do not present here the corresponding graphical representation). The advantage of this regime is the much better quality of spatial distributions of acoustic and temperature fields, and its disadvantage is the more than twofold increase in the duration of ultrasonic treatment that is necessary for obtaining the same thermal effect.

The results presented above show that arrays with random element distributions provide a noticeably better quality of intensity and temperature distributions in the case of the steering of several foci than arrays with regular element distributions. We determined the parameters of a random array, the geometry of the arrangement of nine foci, and the heating regime that provide a uniform thermal ablation of tissue within the volume surrounding the foci. At the same time, in the field of a regular array, the ablation is observed in both the region of focusing of the set of nine foci and in the region of secondary intensity peaks, which is inadmissible for practical use.

ACKNOWLEDGMENTS

This work was supported by the Russian Foundation for Basic Research, project nos. 02-02-16999 and 03-02-16232, and by the Civil Research and Development Foundation, grant no. PR2-2384-MO-02.

REFERENCES

1. E. S. Ebbini and C. A. Cain, IEEE Trans. Ultrason. Ferroelectr. Freq. Control **36** (5), 540 (1989).
2. X. Fan and K. Hynynen, Ultrasound Med. Biol. **22** (4), 471 (1996).
3. E. Ebbini and C. A. Cain, Int. J. Hyperthermia **7** (6), 951 (1991).
4. X. Fan and K. Hynynen, Phys. Med. Biol. **41** (4), 591 (1996).
5. H. Wan, P. VanBaren, E. S. Ebbini, and C. A. Cain, IEEE Trans. Ultrason. Ferroelectr. Freq. Control **43** (6), 1085 (1996).
6. C. Damianou and K. Hynynen, Ultrasound Med. Biol. **19** (9), 777 (1993).

7. S. A. Goss, L. A. Frizell, J. T. Kouzmanoff, *et al.*, IEEE Trans. Ultrason. Ferroelectr. Freq. Control **43** (6), 1111 (1996).
8. L. R. Gavrilov and J. Hand, IEEE Trans. Ultrason. Ferroelectr. Freq. Control **47** (1), 125 (2000).
9. L. R. Gavrilov and J. W. Hand, Akust. Zh. **46**, 456 (2000) [Acoust. Phys. **46**, 390 (2000)].
10. G. R. ter Haar, Phys. Today **54** (12), 29 (2001).
11. M. I. Skolnik, *Introduction to Radar Systems* (McGraw-Hill, New York, 1962; Mir, Moscow, 1965).
12. E. A. Filonenko, V. A. Khokhlova, and L. R. Gavrilov, in *Proceedings of XI Session of the Russian Acoustical Society* (GEOS, Moscow, 2001), p. 19.
13. H. T. O'Neil, J. Acoust. Soc. Am. **21**, 516 (1949).
14. G. Strang, *Linear Algebra and Its Applications* (Academic, New York, 1980).
15. H. H. Pennes, J. Appl. Physiol. **1**, 93 (1948).
16. J. P. Bensted, Phys. Med. Biol. **38**, 1661 (1993).
17. E. A. Filonenko and V. A. Khokhlova, Akust. Zh. **47**, 541 (2001) [Acoust. Phys. **47**, 468 (2001)].
18. S. A. Sapareto and W. C. Dewey, Radiat. Oncol. Biol. Phys. **10**, 787 (1984).
19. C. Damianou, K. Hynynen, and X. Fan, in *Proceedings of IEEE International Ultrasonics Symposium* (1993), p. 1199.
20. D. R. Daum and K. Hynynen, IEEE Trans. Ultrason. Ferroelectr. Freq. Control **46** (5), 1254 (1999).

Translated by M. Lyamshev